Vector Network Analyser-based Terahertz Solution for High-quality Medical Imaging

Hanya T. Ahmed[1], Robert C. Jones, Rostyslav Dubrovka, Robert Donnan, Akram Alomainy
[1]London, United Kingdom

***Abstract*— This paper introduces a comparative evaluation between Terahertz (THz) imaging (based on a Vector Network Analyzer (VNA)), and Optical Coherence Tomography (OCT). The use of the VNA is assessed in suppressing the issue of speckle noise introduced in OCT imaging, which hinders clinical interpretation. Depth profiles of the sample (A-Scans) were produced by both systems which, when stacked, build a B-scan image. Each system was visually evaluated by its ability to spatially resolve both along and normal to the beam axis, using a phantom resembling a tooth with a hole, including a lattice structure representing decay. Relative to commonly appreciated x-ray imaging, results show that comparatively VNA-based imaging can be done to greater spatial resolution than with infrared OCT.**

I. Introduction

OPTICAL Coherence Tomography (OCT) is a recent and growing imaging technology based on low-coherence interferometry to acquire backscattered light [1]. It is widely developed in the medical field, specifically in ophthalmology and dentistry [2, 3]. Its distinctive virtues are use of non-ionising probe radiation and comparatively inexpensive implementation (c.f., X-ray) [4]. Even so, the common Michaelson interferometric configuration of OCT suffers speckle noise, inherent in the characteristic low coherence of its light source.

Similarly, THz imaging has been demonstrating its recent potential in the medical field over the past decade or so [5]. Like OCT, THz imaging is non-ionising; it also has a similar skin penetration depth of 0.1– 0.3 mm into human tissue. But unlike OCT, THz light, as available in a coherent transceiver system (such as a VNA), is consequently less immune to speckle noise [6].

II. Methodology

In this paper, a swept-source OCT (SS-OCT) via a Michaelson interferometer, was implemented. Its source has a centre-wavelength of 1310 nm and bandwidth of 75 nm. The VNA was coupled to a bi-static quasi-optical circuit that consisted of a Tx/Rx pair of corrugated horns operating over the band of 220-325 GHz. The circuit consists of a symmetric arrangement of four fixed, beam-shaping, mirrors with the sample placed for transmission (Fig 1). An image is built by translating the sample, alone, in a plane normal to the beam axis.

OCT records a spectral interferogram which is analysed via an inverse Fourier transform (IFT) to yield A-scans that are depth profiles which, when stacked, build a B-scan image. Conversely, the VNA records the complex amplitude reflectance (S_{11}) or transmittance (S_{21}). S-parameter analysis renders A-scans through an Inverse Fast Fourier Transform (IFFT) (transforming from frequency- to time-domain). Comparison of analyses will highlight the advantage of imaging with a coherent transceiver system.

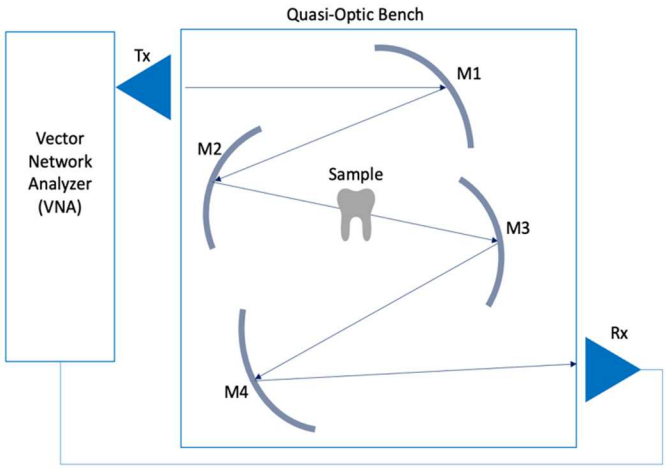

Fig. 1. Experimental transmission setup implemented using the Vector Network Analyzer (VNA). A quasi-optic bench supported four fixed, profiled mirrors, in which M2 and M3 are fast-focusing paraboloids and M1 and M4 are off-axis ellipsoids.

III. Phantom

The phantom imaged in these experiments is a 3D printed representation of a human tooth that, for present instrument restrictions, is enlarged to enable imaging by the VNA. It was 3D printed by the Formlabs Form 2 3D printer with a castable wax that is a photopolymer resin, chosen for its refractive index of 1.53 [7]; the refractive index of enamel and dentin are, respectively, nominally 1.63 and 1.54 [8]. The phantom was designed to present decay, as represented by a cavity (see Fig 2a), together with a lattice structure within the hole.

The imaging process started from point 1 to 50 shown in Fig

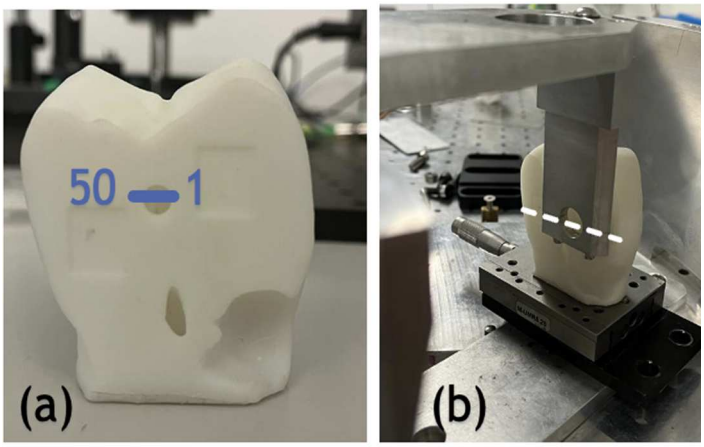

Fig. 2. a) Displays the phantom imaged by both OCT and VNA, in which it is imaged from point 1 to point 50 in steps of 0.3mm in the x-direction. b) Shows the phantom placed between M3 and M4 for transmission setup, so that the focusing slot is aimed at point 1 in the beginning.

2a, where for transmission, the phantom was placed between shaped-mirrors, M3 and M4 (Fig 2b). Thus, point 1 was positioned at the focus slot then moved in the x-axis direction in 0.3 mm steps to obtain S_{21} spectral values for each X position. For each step and frequency a value of $X_{n+1} - X_n$ was computed to obtain the magnitude and phase data for the 0.3mm step. This was done to simulate more pixels from a large beam width relative to the hole in the phantom. Further processing was performed to obtain an equivalent B-Scan from S_{21} values. This included processing both magnitude and phase at each frequency to produce an A-scan of the frequency sweep at each X position. $|S_{21}|$ ('Mangitude' in Fig. 3), shows the strength of signal for a given X, and phase is related to the electrical path length experienced at X and so sensitive to the depth of the decay in the phantom. Figure 3 therefore shows a dispersive image built from plotting, for each X, the signal magnitude.

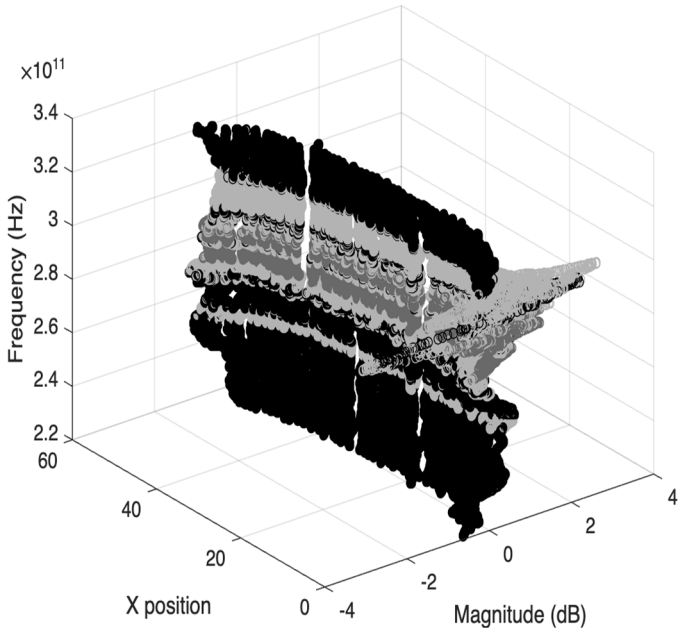

Fig. 3. VNA results of the phantom from position X = 1 to X = 50, in which the x-axis is the magnitude in dB, the y-axis is position X and, z-axis is frequency. The greyscale depicts the phase. Lighter shades are associated with X further from the zero-phase reference.

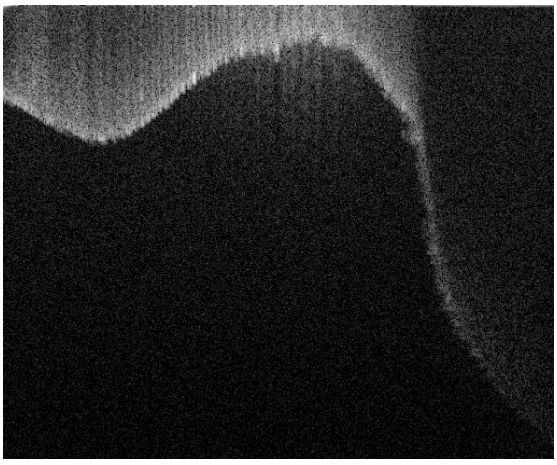

Fig. 4. A B-scan OCT image of the phantom built from A scans covering X: 1 - 50. Note that the OCT cannot image the whole depth. Additionally, speckle noise blurs the outline of the hole since. Further, the lattice structure associated with the hole is not resolved.

Phase is represented via the grayscale and correlates to OCT the image of Fig. 4, so that the zero-phase reference is the darkest shade possible (black).

IV. Results

These experiments present raw initial results for imaging a phantom produced to compare OCT and VNA for decay detection. For VNA imaging, Fig. 3 renders the equivalent to an OCT B-scan with reduced noise (i.e. speckle and blur), and greater depth of signal penetration; note that the OCT B-scan of Fig. 4 shows OCT unable to image to the full depth at each X. Commensurate with an operating waveband of 220 - 325 GHz the VNA proved able to resolve mm/sub-mm-scale features in the phantom. OCT also added a significant amount of speckle noise in the form of motion artifacts. This is clearly visible above the layer of phantom in Fig 4.

V. Conclusion

THz imaging via a Vector Network Analyzer (VNA) was compared to Optical Coherence Tomography (OCT) imaging for dentistry application. OCT images manifested the characteristic speckle noise inherent in its interferometry with low coherence light. Using a VNA, the tooth-phantom is placed in a transmission setup and S_{21} analysis was performed to simulate a B-scan to mimic an OCT image. A dispersive complex signal amplitude was measured at successive A-scan points (as for the OCT). In the configuration used, VNA resolved to 0.3 mm and could locate the region of decay. Further work will translate the VNA procedure to 0.5 – 1.0 THz with a phantom supporting other features of decay.

References

[1] M.A. Choma, M.V. Sarunic, C. Yang and J.A. Izzat, "Sensitivity advantage of swept source and Fourier domain optical coherence tomography," *Optics Express*, vol. 11, no. 18, pp. 2183-2189, 2003.

[2] C. Cukras, Y.D. Wang, C.B.Meyerle, F.Forooghian, E.Y.Chew and W.T.Wong, "Optical coherence tomography-based decision making in exudative age-related macular degeneration: comparison of time- vs spectral-domain devices," *Eye*, vol. 24, no. 5, pp. 775-783, 2010.

[3] N. Karimian, H. S. Salehi, M. Mahdian, H. Alnajjar and A. Tadinada, "Deep learning classifier with optical coherence tomography images for early dental caries detection," *Proc. S PIE 10473 Lasers in Dentistry XXIV*, p. 1047304, 8 February 2018.

[4] J. M. Schmitt, S. H. Xiang and K. M. Yung, "Speckle in optical coherence tomography," *Journal of Biomedical Optics*, vol. 4, no. 1, 1999.

[5] F. R. Faridi and S. Preu, "Characterization of a Crossed Dipole Resonator Array using a Pulsed Free Space Two-Port Photonic VNA," *International Conference on Infrared, Millimeter and Terahertz Waves (IRMMW-THz),*2021.

[6] B. Yang, H. Su, R. S. Donnan, "Vector network analysis of dielectric and magnetic materials in the millimetre wave band," *Journal of Physics: Conference Series,* vol. 286, no.1, pp. 012019, 2011.

[7] M. Reynoso, I. Gauli, and P. Measor, "Refractive index and dispersion of transparent 3D printing photoresins", *Optical Materials Express,* vol.11 no. 10, pp. 3392-3397, 2021

[8] Z. Meng, X. S. Yao, H. Yao, Y. Liang, T. Liu, Y. Li, G. Wang, S. Lan, "Measurement of the refractive index of human teeth by optical coherence tomography," *Journal of Biomedical Optics,* vol. 14, no.3, pp. 034010, 2009.